

Quantum metric induced magneto-optical effects in \mathcal{PT} -symmetric antiferromagnets

Yongpan Li,¹ Yichen Liu,¹ and Cheng-Cheng Liu^{1,*}

¹Centre for Quantum Physics, Key Laboratory of Advanced Optoelectronic Quantum Architecture and Measurement (MOE), School of Physics, Beijing Institute of Technology, Beijing, 100081, China

The magneto-optical effects (MOEs), as a fundamental physical phenomenon, can reveal the electronic structures of materials. The related probing methods are widely used in the study of magnetic materials. However, space-time inversion (\mathcal{PT}) symmetric antiferromagnets were previously believed to be magneto-optically inactive. Here, we point out that this traditional understanding is incorrect. Based on our generic formulas and symmetry analysis, we find that in \mathcal{PT} -symmetric antiferromagnets, it is the quantum metric, i.e., the real part of the quantum geometry, that induces MOEs. Combining a tight-binding model and first-principles calculations, we confirm this observation by showing MOEs in the \mathcal{PT} -symmetric antiferromagnet. Our work demonstrates that \mathcal{PT} -symmetric antiferromagnets previously thought to lack MOEs can indeed exhibit MOEs and greatly broaden the research on MOEs.

Introduction.—The magneto-optical effects (MOEs) in magnetic materials have been a long-standing research focus [1–19]. When light is incident on a magnetic material, both the reflection and transmission of the light at the surface, as well as the propagation of the light inside the material, can be characterized by its frequency and complex refractive index. The fundamental physics underlining various MOEs is that the two eigenmodes of the magnetic material have different complex refractive indices. Given the material-specific dielectric tensor ϵ and permeability tensor μ , we can obtain the complex refractive indices by solving the wave equation. Since one can assume $\mu = 1$ at optical and near-infrared frequencies [20, 21] and the optical conductivity tensor σ can be converted into the dielectric tensor ϵ [22, 23], to study MOEs, it amounts to investigate optical conductivity tensor σ of magnetic materials.

The conventional understanding holds that the vanishing off-diagonal term of the optical conductivity tensor σ would result in the disappearance of magneto-optical effects, as in the case of the Kerr effect, where the Kerr angle is given by $\theta_K = -\sigma_{xy}/(\sigma_{xx}\sqrt{1+i\sigma_{xx}/\omega\epsilon_0})$ [24, 25]. Based on this understanding, the space-time inversion (\mathcal{PT}) symmetric antiferromagnets with vanishing Berry curvature are magneto-optically inactive. With the introduction of the quantum geometry [26–34] in recent years, we have gained a more comprehensive understanding of the optical conductivity [35–40]. The quantum geometry is a multiband effect, so for the optical conductivity related to quantum geometry, only interband transitions are relevant [26, 29, 41–43]. However, the significance of the quantum metric, i.e., the real part of the quantum geometry, in MOEs has not been appreciated.

In this work, we study the magneto-optical Kerr and Faraday effects in \mathcal{PT} -symmetric antiferromagnets. Our symmetry analysis shows that in such systems, only the quantum metric contributes to the optical conductivity tensor. We derive the universal formulas without assuming any symmetry for the complex refractive indices. Based on the complex refractive indices, the generic for-

mulas involving quantum metric for Kerr and Faraday effects in three-dimensional (3D) and two-dimensional (2D) \mathcal{PT} -symmetric systems are given. Using a tight-binding model and first-principles calculations, we show that the quantum metric can solely induce large MOEs without the Berry curvature.

Formulas and symmetry analysis.—The complex refractive indices of the eigenmodes of a magnetic material can be obtained by solving the wave equations. When light is incident along the normal direction to the surface, typically, there should be two different eigenmodes, and the complex refractive indices n_{\pm} of the two eigenmodes are given by [Supplementary Material (SM) [44] Sec. II]

$$n_{\pm}(\omega) = \sqrt{\frac{(\epsilon_{xx} + \epsilon_{yy}) \pm \sqrt{(\epsilon_{xx} - \epsilon_{yy})^2 + 4\epsilon_{xy}\epsilon_{yx}}}{2}}, \quad (1)$$

where $\hbar\omega$ is the photon energy, and ϵ is the permittivity tensor and implicitly depends on ω . The relation between permittivity tensor ϵ and the optical conductivity tensor σ is $\epsilon_{ij} = \delta_{ij} + i\sigma_{ij}/\epsilon_0\omega$. Our formulas are more universal than the previous formulas since we assume no symmetry and make no approximations, like cubic symmetry [22, 23], as well as $\sigma_{xx} \gg \sigma_{xy}$ in typical cases [22, 23] and $\sigma_{xx} \ll \sigma_{xy}$ in topological magnetic thin films [45, 46].

The components of the optical conductivity tensor σ read [38]

$$\sigma_{ab}(\omega) = -\frac{ie^2}{\hbar} \sum_{n \neq m} \int \frac{d^3k}{(2\pi)^3} (f_{n\mathbf{k}} - f_{m\mathbf{k}}) \times \omega_{nm\mathbf{k}} \frac{r_{nm\mathbf{k}}^a r_{m\mathbf{k}}^b}{\omega_{nm\mathbf{k}} + \omega + i\eta}. \quad (2)$$

$f_{n\mathbf{k}}$ is the Fermi-Dirac distribution function, $\hbar\omega_{nm\mathbf{k}}$ is the energy difference between the n th band and m th band at the same \mathbf{k} point, and $\eta > 0$ is a smearing parameter. The term $r_{nm\mathbf{k}}^a r_{m\mathbf{k}}^b$ is the components of the quantum geometry tensor \mathbf{Q} [26, 41, 42, 47], which can be rewritten

TABLE I. Symmetry-imposed form of the optical conductivity tensor σ . Without loss of generality, we consider light incident along the positive z -direction on a surface lying in the xy -plane. NS denotes no symmetry constraint, and \mathcal{O} refers to three-fold or higher rotational symmetry. The contributions from the quantum metric and Berry curvature are denoted as σ_{ij}^g and σ_{ij}^Ω according to Eq. (4), respectively.

NS	\mathcal{PT}	\mathcal{O}
$\begin{pmatrix} \sigma_{xx}^g & \sigma_{xy}^g + \sigma_{xy}^\Omega \\ \sigma_{xy}^g - \sigma_{xy}^\Omega & \sigma_{yy}^g \end{pmatrix}$	$\begin{pmatrix} \sigma_{xx}^g & \sigma_{xy}^g \\ \sigma_{xy}^g & \sigma_{yy}^g \end{pmatrix}$	$\begin{pmatrix} \sigma_{xx}^g & \sigma_{xy}^\Omega \\ -\sigma_{xy}^\Omega & \sigma_{xx}^g \end{pmatrix}$

as

$$Q_{nmk}^{ab} := r_{nmk}^a r_{nmk}^b \equiv g_{nmk}^{ab} - \frac{i}{2} \Omega_{nmk}^{ab}, \quad (3)$$

with g_{nmk}^{ab} and Ω_{nmk}^{ab} being the components of the quantum metric tensor and Berry curvature tensor, respectively. Therefore, the transverse optical conductivity σ_{xy} can be rewritten as [SM Sec. I]

$$\begin{aligned} \sigma_{xy}(\omega) &= \sum_{n \neq m} \int \frac{d^3k}{(2\pi)^3} \left(\frac{2ie^2}{\hbar} \frac{f_{nk}\omega\omega_{mnk}}{\omega_{mnk}^2 - (\omega + i\eta)^2} g_{nmk}^{xy} \right. \\ &\quad \left. - \frac{e^2}{\hbar} \frac{f_{nk}\omega_{mnk}^2}{\omega_{mnk}^2 - (\omega + i\eta)^2} \Omega_{nmk}^{xy} \right) \\ &\equiv \sigma_{xy}^g + \sigma_{xy}^\Omega, \end{aligned} \quad (4)$$

where σ_{xy}^g represents the contribution from the quantum metric g_{nmk}^{xy} and σ_{xy}^Ω represents the contribution from the Berry curvature Ω_{nmk}^{xy} .

The Berry curvature Ω_{nmk}^{ab} transforms as $\Omega_{nmk}^{ab} = -\Omega_{nmk}^{ab}$ under \mathcal{PT} -symmetry. So, for \mathcal{PT} -symmetric antiferromagnets, the Berry curvature is zero everywhere in the Brillouin zone (BZ), and the optical conductivity is purely contributed by the quantum metric. One should be careful that the mirror symmetry M_x or M_y and two-fold rotational symmetry C_{2x} or C_{2y} can forbid the transverse optical conductivities, i.e., σ_{xy} and σ_{yx} [SM Sec. I]. Therefore, the direction of the electric field of the incident light should neither lie in nor be perpendicular to the mirror plane and should also neither align with nor be perpendicular to the two-fold rotation axis.

The quantum metric g_{nmk}^{xy} and the Berry curvature Ω_{nmk}^{xy} are symmetric and antisymmetric under exchange of x and y , respectively, i.e., $g_{nmk}^{xy} = g_{nmk}^{yx}$ and $\Omega_{nmk}^{xy} = -\Omega_{nmk}^{yx}$. σ_{xy}^g and σ_{xy}^Ω obey the same symmetry restrictions as the quantum metric and Berry curvature, i.e., $\sigma_{xy}^g = \sigma_{yx}^g$ and $\sigma_{xy}^\Omega = -\sigma_{yx}^\Omega$. However, three-fold or higher rotational symmetry imposes constrictions on the form of the optical conductivity tensor [48], i.e., $\sigma_{xx}^{g/\Omega} = \sigma_{yy}^{g/\Omega}$ and $\sigma_{xy}^{g/\Omega} = \sigma_{yx}^{g/\Omega}$. Therefore, in this case, the quantum metric makes no contribution to the transverse optical conductivity σ_{xy} and σ_{yx} [SM Sec. I]. The symmetry analysis above is summarized in Table I.

For 3D \mathcal{PT} -symmetric antiferromagnets, the specific Faraday angle $\theta_F/l = \theta_F/l + i\xi_F/l$ and the Kerr angle $\tilde{\theta}_K = \theta_K + i\xi_K$ are given by [SM Sec. II]

$$\tilde{\theta}_F = \left(-N + \sqrt{N^2 + 1} \frac{e^{ik_0 n_+ l} + e^{ik_0 n_- l}}{e^{ik_0 n_+ l} - e^{ik_0 n_- l}} \right)^{-1}, \quad (5)$$

$$\tilde{\theta}_K = \left(-N + \sqrt{N^2 + 1} \frac{n_+ n_- - 1}{n_+ - n_-} \right)^{-1}. \quad (6)$$

l is the propagation distance of the light and $N = (\epsilon_{yy} - \epsilon_{xx})/2\epsilon_{xy}$. For 2D \mathcal{PT} -symmetric systems, the Faraday angle $\tilde{\theta}_F = \theta_F + i\xi_F$ and the Kerr angle $\tilde{\theta}_K = \theta_K + i\xi_K$ can be written as

$$\tilde{\theta}_F = \left(-N + \sqrt{N^2 + 1} \frac{t(n_+) + t(n_-)}{t(n_+) - t(n_-)} \right)^{-1}, \quad (7)$$

$$\tilde{\theta}_K = \left(-N + \sqrt{N^2 + 1} \frac{r(n_+) + r(n_-)}{r(n_+) - r(n_-)} \right)^{-1}. \quad (8)$$

$t(n_i)$ and $r(n_i)$ are the total complex transmission coefficient and the total complex reflection coefficient, respectively, and strongly depend on the shape of the sample and substrate. In SM Sec. III, we provide expressions for $t(n_i)$ and $r(n_i)$ in a relatively simpler case. When the system exhibits three-fold or higher rotational symmetry, our formulas for the 3D systems can reduce to the commonly known forms [24, 25], and a detailed discussion is given in SM Sec. II.

Tight-binding model.—We now consider a 3D honeycomb lattice with collinear antiferromagnetic order as shown in Fig. 1(a). The Hamiltonian is given by [50, 51]

$$\begin{aligned} H &= -t \sum_{\langle ij \rangle \alpha} c_{i\alpha}^\dagger c_{j\alpha} + it_{\text{SOC}} \sum_{\langle\langle ij \rangle\rangle \alpha \beta} \nu_{ij} c_{i\alpha}^\dagger \sigma_{\alpha\beta}^z c_{j\beta} \\ &\quad - t_z \sum_{i\alpha} \left(c_{i\alpha}^\dagger c_{i+z,\alpha} + c_{i\alpha}^\dagger c_{i-z,\alpha} \right) \\ &\quad + \sum_{i\alpha\beta} (-1)^i m c_{i\alpha}^\dagger s_{\alpha\beta}^z c_{i\beta}, \end{aligned} \quad (9)$$

where i, j denote sublattice degree of freedom and α, β label spin degree of freedom. The first term is the intralayer nearest-neighbor hopping term. The second term is the effective intrinsic spin-orbit coupling (SOC) term. $\nu_{ij} = \mathbf{d}_i \times \mathbf{d}_j / |\mathbf{d}_i \times \mathbf{d}_j|$, where \mathbf{d}_i and \mathbf{d}_j are two nearest bonds connecting the next-nearest neighbors i and j . The third term is the interlayer nearest-neighbor hopping term in the z direction. The last term denotes the antiferromagnetic order.

When all intralayer nearest-neighbor hoppings are the same, i.e., $t_1 = t_2 = t_3$ in Fig. 1(a), the system possesses three-fold rotation symmetry C_{3z} . Any magneto-optic effects are forbidden since C_{3z} suppresses the contribution from the quantum metric and \mathcal{PT} suppresses the

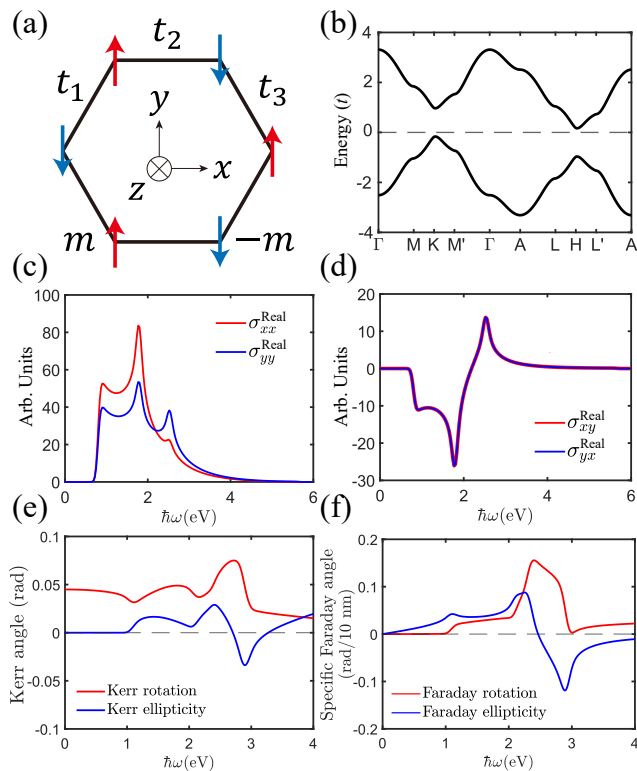


FIG. 1. The magneto-optical effects in generic \mathcal{PT} -symmetric antiferromagnets. (a) Schematic of the tight-binding model. The red up and blue down arrows denote up and down spins, respectively. The \mathcal{PT} symmetry exchanges spin on different sublattices. (b) Energy bands of the tight-binding model. (c) The real part of the diagonal terms of the optical conductivity tensor, σ_{xx} and σ_{yy} . (d) The real part of the off-diagonal terms of the optical conductivity tensor with $\sigma_{xy} = \sigma_{yx}$. In (c) and (d), as explained in the text, the imaginary part can be obtained from the corresponding real part through the Kramers-Kronig relation. (e) The complex Kerr angle $\tilde{\theta}_K = \theta_K + i\xi_K$ is shown in terms of the Kerr rotation θ_K and Kerr ellipticity ξ_K . (f) The specific Faraday angle $\tilde{\theta}_F/l = \theta_F/l + i\xi_F/l$ is shown in terms of the Faraday rotation θ_F and Faraday ellipticity ξ_F per unit thickness l with $l=10$ nm. Parameters: $t_1 = 0.8t$, $t_2 = t_3 = 1.0t$, $t_z = 0.2t$, $m = 0.8t$, $t_{\text{SOC}} = 0.05t$, and the smearing parameter is set to $0.04t$.

contribution from the Berry curvature. Therefore, we introduce the uniaxial strain to make $t_1 \neq t_2 = t_3$, i.e., breaking three-fold rotational symmetry while keeping inversion symmetry.

After applying the uniaxial strain, the system still has \mathcal{PT} -symmetry, leading to Kramers degeneracy in all bands as shown in Fig. 1(b). In Fig. 1(c) and Fig. 1(d), the real parts of the diagonal (σ_{xx} and σ_{yy}) and off-diagonal (σ_{xy} and σ_{yx}) terms of the optical conductivity tensor are shown, respectively. The difference between σ_{xx} and σ_{yy} explicitly shows the broken of three-fold rotational symmetry and the nonzero and equal σ_{xy} and σ_{yx} are purely contributed by the quantum metric. Since

the optical conductivity tensor is contributed purely by the quantum metric, the real part and the imaginary part of the optical conductivity tensor are just the Hermitian part and anti-Hermitian part of the optical conductivity tensor, respectively [SM Sec. IV]. Therefore, the imaginary part can be obtained from the corresponding real part through the Kramers-Kronig relation.

The complex Kerr and Faraday angles are shown in Figs. 1(e) and (f), respectively. When the energy of the photon is smaller than the minimum value of the local gap, there is no Faraday rotation and Kerr ellipticity, while Kerr rotation and Faraday ellipticity are finite. This is opposite to the systems with three-fold or higher rotational symmetry, where there is no Kerr rotation and Faraday ellipticity while Faraday rotation and Kerr ellipticity are finite [22]. The reason is that when the optical conductivity tensor is purely contributed by the quantum metric, the two eigenmodes of the system are linearly polarized light with electric field directions perpendicular to each other. However, when the system has three-fold or higher rotational symmetry, the two eigenmodes become left- and right-circularly polarized light. When calculating the Faraday and Kerr angles by computing the ratio $E_y/E_x = \theta + i\xi$ [SM Sec. II], the circularly polarized light will have an additional phase difference $e^{i\pi/2}$ compared to the linearly polarized light, thus leading to swapping of rotation and ellipticity.

Materials.—Using the first-principles method, we show the magneto-optical Kerr and Faraday effects in generic \mathcal{PT} -symmetric antiferromagnets. Here, we take two illustrative \mathcal{PT} -symmetric antiferromagnetic materials, i.e., 3D CoAgPO₄ [52] (ICSD 100520) and 2D bilayer CrI₃ [7] subjected to uniaxial strain, as examples.

The crystal structure of experimentally prepared CoAgPO₄ is shown in Fig. 2(a), and the space group of CoAgPO₄ without magnetism is $P\bar{1}$. When the magnetism is taken into account, the inversion symmetry interchanges two Co atoms with opposite magnetic moments, and thus the system possesses \mathcal{PT} symmetry. The band structure is shown in Fig. 2(b), which has a gap of about 1.7 eV. The components of the optical conductivity tensor are shown in Fig. 2(c). To quantify the MOEs, we calculate the Kerr angle and specific Faraday angle as shown in Fig. 2(d). For the Kerr effect, the 3D CoAgPO₄ exhibits a large Kerr rotation of about 43 mrad at 4.4 eV and a large Kerr ellipticity of about 45 mrad at 3.5 eV. For the Faraday effect, the 3D CoAgPO₄ exhibits a large specific Faraday rotation of about 101 mrad per 100 nm at 3.5 eV and a large specific Faraday ellipticity of about 99 mrad per 100 nm at 4.4 eV.

The monolayer CrI₃ is a ferromagnet and possesses three-fold rotation symmetry. However, the bilayer CrI₃, which also has three-fold rotational symmetry, is an antiferromagnet [7]. To break the three-fold rotational symmetry, we apply an uniaxial strain to the bilayer CrI₃. The uniaxial strain that does not break the inversion

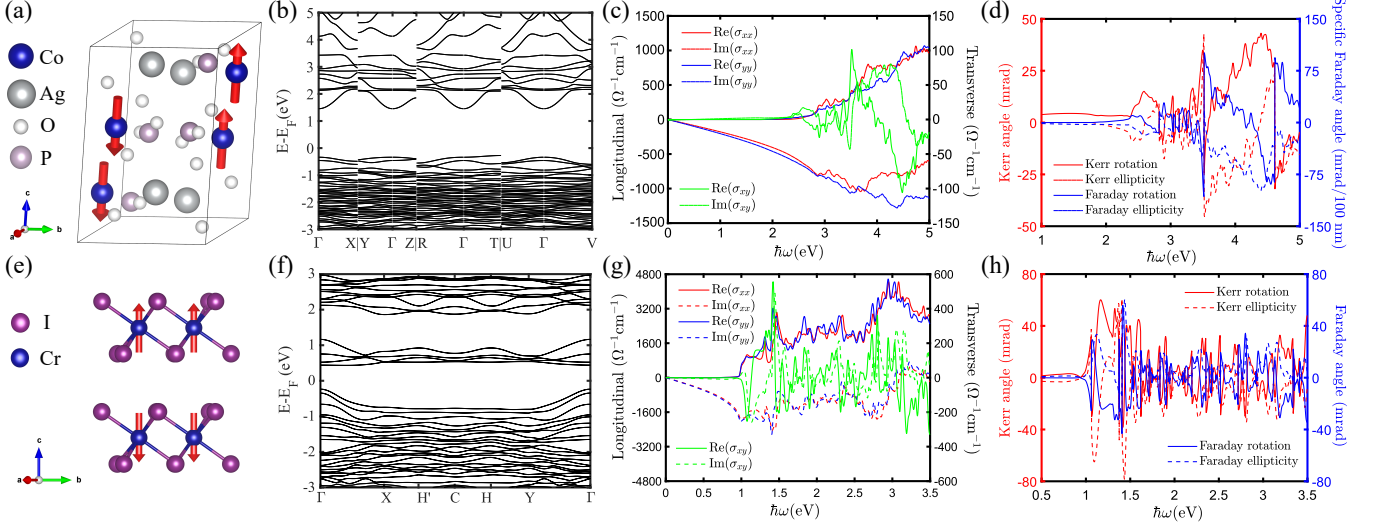


FIG. 2. The magneto-optical Kerr and Faraday effects induced purely by the quantum metric in real materials. (a) Crystal structure of CoAgPO_4 . The crystal structure is drawn using VESTA [49]. (b) The band structure of CoAgPO_4 . (c) The components of the optical conductivity tensor of CoAgPO_4 . The longitudinal conductivities, i.e., σ_{xx} and σ_{yy} , correspond to the left y -axis, while the transverse conductivity, i.e., $\sigma_{xy} = \sigma_{yx}$, corresponds to the right y -axis. (d) The complex Kerr angle (left y -axis) and the specific complex Faraday angles (right y -axis). (e) Crystal structure of strained bilayer CrI_3 . (f) The band structure of strained bilayer CrI_3 . (g) The components of the optical conductivity tensor of the strained bilayer CrI_3 . (h) The complex Kerr angle $\tilde{\theta}_K$ (left y -axis) and the complex Faraday angles $\tilde{\theta}_F$ (right y -axis).

symmetry can induce the quantum metric and MOEs in 2D magnetic materials.

Here, we compress one axis of the bilayer CrI_3 by 3%, and the crystal structure is shown in Fig. 2(e). After applying the uniaxial strain, the space group of the bilayer CrI_3 without considering magnetism becomes $P\bar{1}$. The band structure is shown in Fig. 2(f), which has a gap of about 0.67 eV. The components of the optical conductivity tensor are shown in Fig. 2(g). The Kerr and Faraday angles are shown in Fig. 2(h). For the Kerr effect, the 2D strained bilayer CrI_3 exhibits a large Kerr rotation of about 60 mrad at 1.2 eV and a large Kerr ellipticity of about 78 mrad at 1.4 eV. For the Faraday effect, the 2D strained bilayer CrI_3 exhibits a large Faraday rotation of about 56 mrad and Faraday ellipticity of about 61 mrad at 1.4 eV.

Since both CoAgPO_4 and strained bilayer CrI_3 have \mathcal{PT} -symmetry, there is no contribution from Berry curvature in the optical conductivity tensor. As the optical conductivity tensor is solely induced by the quantum metric, these MOEs are also solely induced by the quantum metric. As can be seen from the Figs. 2(d) and (h), in real materials, the quantum metric can fully induce large MOEs without the Berry curvature.

Discussion.—Compared to 2D \mathcal{PT} -symmetric antiferromagnets with high rotational symmetry, the counterparts with low rotational symmetry are less. However, one can break the high rotational symmetry of 2D \mathcal{PT} -symmetric antiferromagnets through various tuning methods, and the quantum metric-induced MOEs can

still be expected in these materials. On one hand, the high rotational symmetry can be broken by applying strain, such as using lattice-mismatched substrates, unusually shaped substrates, or substrates with piezoelectric effects to induce strain. On the other hand, for \mathcal{PT} -symmetric antiferromagnetic bilayer materials with high rotational symmetry, introducing interlayer sliding can misalign the rotational axes and break the corresponding rotational symmetry. For instance, while the bilayer CrI_3 has been previously measured to be magneto-optically inactive [7], our theory predicts that applying a small strain or interlayer sliding could induce significant MOEs. Given the diversity of 2D magnetic materials, such as bilayer CrI_3 , the increasingly advanced tuning techniques, and the well-established methods for measuring MOEs, our proposed quantum metric-induced MOEs can be readily achieved and observed experimentally within current material systems and experimental conditions.

Previously, the role of the quantum metric in MOEs had not been recognized and the symmetry of MOEs was regarded as equivalent to the symmetry of Berry curvature. Our work demonstrates that in the \mathcal{PT} -symmetric antiferromagnets, one must consider the contribution from the quantum metric. It should be noted that even for 3D \mathcal{PT} -symmetric antiferromagnets with three-fold or higher rotational symmetry, the quantum metric-induced MOEs remain active when light is incident on their low-symmetry surfaces. Therefore, many materials previously thought to lack MOEs, such as

\mathcal{PT} -symmetric antiferromagnets, actually exhibit MOEs. Our work reveals purely quantum metric-induced MOEs in \mathcal{PT} -symmetric antiferromagnets and greatly deepens the understanding of MOEs.

Acknowledgments.—The work is supported by the NSF of China (Grant No. 12374055), the National Key R&D Program of China (Grant No. 2020YFA0308800), and the Science Fund for Creative Research Groups of NSFC (Grant No. 12321004). Yongpan Li and Yichen Liu contribute equally to the work.

* ccliu@bit.edu.cn

- [1] J. L. Erskine and E. A. Stern, *Phys. Rev. Lett.* **30**, 1329 (1973).
- [2] J. L. Erskine and E. A. Stern, *Phys. Rev. B* **8**, 1239 (1973).
- [3] T. Kato, H. Kikuzawa, S. Iwata, S. Tsunashima, and S. Uchiyama, *J. Magn. and Magn. Mater.* **140-144**, 713 (1995).
- [4] G. Y. Guo and H. Ebert, *Phys. Rev. B* **51**, 12633 (1995).
- [5] H. Chen, Q. Niu, and A. H. MacDonald, *Phys. Rev. Lett.* **112**, 017205 (2014).
- [6] W. Feng, G.-Y. Guo, J. Zhou, Y. Yao, and Q. Niu, *Phys. Rev. B* **92**, 144426 (2015).
- [7] B. Huang, G. Clark, E. Navarro-Moratalla, D. R. Klein, R. Cheng, K. L. Seyler, D. Zhong, E. Schmidgall, M. A. McGuire, D. H. Cobden, *et al.*, *Nature* **546**, 270 (2017).
- [8] M. Wu, H. Isshiki, T. Chen, T. Higo, S. Nakatsuji, and Y. Otani, *Appl. Phys. Lett.* **116**, 132408 (2020).
- [9] Z.-B. Hu, L.-H. Li, Y. Han, J. Zhang, J. Li, Z. Chen, S. Wu, Y. Zhang, H.-Y. Ye, and Y. Song, *Aggregate* **4**, e294 (2023).
- [10] Z. Khaghani, M. Hosseini Farzad, and A. Asgari, *Opt. Quant. Electron.* **54**, 645 (2022).
- [11] I. Lyalin, S. Alikhah, M. Berritta, P. M. Oppeneer, and R. K. Kawakami, *Phys. Rev. Lett.* **131**, 156702 (2023).
- [12] F. Johnson, J. Zázvorka, L. Beran, D. Boldrin, L. F. Cohen, J. Zemen, and M. Veis, *Phys. Rev. B* **107**, 014404 (2023).
- [13] T. Nomoto, S. Minami, Y. Yanagi, M.-T. Suzuki, T. Koretsume, and R. Arita, *Phys. Rev. B* **109**, 094435 (2024).
- [14] T. Yin, K. A. Ulman, S. Liu, A. Granados del Águila, Y. Huang, L. Zhang, M. Serra, D. Sedmidubsky, Z. Sofer, S. Y. Quek, *et al.*, *Adv. Mater.* **33**, 2101618 (2021).
- [15] J. Ahn, S.-Y. Xu, and A. Vishwanath, *Nat. Commun.* **13**, 7615 (2022).
- [16] Y. Xu, Z. Ni, Y. Liu, B. R. Ortiz, Q. Deng, S. D. Wilson, B. Yan, L. Balents, and L. Wu, *Nat. Phys.* **18**, 1470 (2022).
- [17] S. Xia, D. O. Ignatyeva, Q. Liu, J. Qin, T. Kang, W. Yang, Y. Chen, H. Duan, L. Deng, D. Long, *et al.*, *ACS Photonics* **9**, 1240 (2022).
- [18] Y. D. Kato, Y. Okamura, M. Hirschberger, Y. Tokura, and Y. Takahashi, *Nat. Commun.* **14**, 5416 (2023).
- [19] X. Li, C. Liu, Y. Zhang, S. Zhang, H. Zhang, Y. Zhang, W. Meng, D. Hou, T. Li, C. Kang, *et al.*, *Nat. Phys.* **20**, 1145 (2024).
- [20] L. D. Landau and E. M. Lifshitz, *Electrodynamics of Continuous Media* (Pergamon Press, 1961).
- [21] P. S. Pershan, *J. Appl. Phys.* **38**, 1482 (1967).
- [22] K.H.J. Buschow and E.P. Wohlfarth, *Handbook of Ferromagnetic Materials* (North Holland, 1990).
- [23] W. Kuch, R. Schäfer, P. Fischer, and F. U. Hillebrecht, *Magnetic Microscopy of Layered Structures* (Springer Berlin, Heidelberg, 2014).
- [24] W. Voigt, *Magneto-und elektrooptik*, 3 (BG Teubner, 1908).
- [25] F. J. Kahn, P. S. Pershan, and J. P. Remeika, *Phys. Rev.* **186**, 891 (1969).
- [26] J. Ahn, G.-Y. Guo, N. Nagaosa, and A. Vishwanath, *Nat. Phys.* **18**, 290 (2022).
- [27] Y. Gao, S. A. Yang, and Q. Niu, *Phys. Rev. Lett.* **112**, 166601 (2014).
- [28] F. De Juan, A. G. Grushin, T. Morimoto, and J. E. Moore, *Nat. Commun.* **8**, 15995 (2017).
- [29] P. Törmä, S. Peotta, and B. A. Bernevig, *Nat. Rev. Phys.* **4**, 528 (2022).
- [30] D. Kaplan, T. Holder, and B. Yan, *Phys. Rev. Lett.* **132**, 026301 (2024).
- [31] T. Liu, X.-B. Qiang, H.-Z. Lu, and X. C. Xie, *Natl. Sci. Rev.*, nwae334 (2024).
- [32] N. Verma and R. Queiroz, *arXiv:2403.07052* (2024), 10.48550/arXiv.2403.07052.
- [33] Y. Onishi and L. Fu, *Phys. Rev. X* **14**, 011052 (2024).
- [34] M. Ezawa, *Phys. Rev. B* **110**, 195437 (2024).
- [35] R. Kubo, *J. Phys. Soc. Jpn.* **12**, 570 (1957).
- [36] C. S. Wang and J. Callaway, *Phys. Rev. B* **9**, 4897 (1974).
- [37] J. E. Sipe and E. Ghahramani, *Phys. Rev. B* **48**, 11705 (1993).
- [38] C. Aversa and J. E. Sipe, *Phys. Rev. B* **52**, 14636 (1995).
- [39] J. E. Sipe and A. I. Shkrebtii, *Phys. Rev. B* **61**, 5337 (2000).
- [40] J. Jia, L. Xiang, Z. Qiao, and J. Wang, *Phys. Rev. B* **110**, 245406 (2024).
- [41] J. P. Provost and G. Vallee, *Commun. Math. Phys.* **76**, 289 (1980).
- [42] Y.-Q. Ma, S. Chen, H. Fan, and W.-M. Liu, *Phys. Rev. B* **81**, 245129 (2010).
- [43] S. Peotta and P. Törmä, *Nat. Commun.* **6**, 8944 (2015).
- [44] See Supplemental Material for more detailed information on (I) Optical conductivity, (II) Faraday and Kerr effects, (III) Faraday and Kerr effects for two-dimensional materials with substrates, (IV) Calculation details, which includes Ref. [6, 20–22, 25, 38, 53–63].
- [45] W.-K. Tse and A. H. MacDonald, *Phys. Rev. Lett.* **105**, 057401 (2010).
- [46] W.-K. Tse and A. H. MacDonald, *Phys. Rev. B* **84**, 205327 (2011).
- [47] A. Shapere and F. Wilczek, *Geometric phases in physics*, Vol. 5 (World scientific, 1989).
- [48] W. H. Kleiner, *Phys. Rev.* **142**, 318 (1966).
- [49] K. Momma and F. Izumi, *J. Appl. Crystallogr.* **44**, 1272 (2011).
- [50] C.-C. Liu, H. Jiang, and Y. Yao, *Phys. Rev. B* **84**, 195430 (2011).
- [51] M. Ezawa, *Phys. Rev. Lett.* **109**, 055502 (2012).
- [52] I. Tordjman, J. Guitel, A. Durif, M. Averbuch, and R. Masse, *Mater. Res. Bull.* **13**, 983 (1978).
- [53] E. Blount, *Solid State Physics*, **13**, 305 (1962).
- [54] W. Wettling, *J. Magn. Magn. Mater.* **3**, 147 (1976).
- [55] S. Tomita, T. Kato, S. Tsunashima, S. Iwata, M. Fujii, and S. Hayashi, *Phys. Rev. Lett.* **96**, 167402 (2006).
- [56] A. Kirilyuk, A. V. Kimel, and T. Rasing, *Rev. Mod.*

- [Phys. **82**, 2731 \(2010\)](#).
- [57] R. Azzam, N. Bashara, and D. Thorburn Burns, *Ellipsometry and polarized light* (North-Holland, Amsterdam, 1987).
- [58] M. Born and E. Wolf, *Principles of optics: electromagnetic theory of propagation, interference and diffraction of light* (Elsevier, 2013).
- [59] M.-H. Kim, G. Acbas, M.-H. Yang, I. Ohkubo, H. Christen, D. Mandrus, M. A. Scarpulla, O. D. Dubon, Z. Schlesinger, P. Khalifah, and J. Cerne, [Phys. Rev. B **75**, 214416 \(2007\)](#).
- [60] G. Kresse and J. Furthmüller, [Phys. Rev. B **54**, 11169 \(1996\)](#).
- [61] A. A. Mostofi, J. R. Yates, Y.-S. Lee, I. Souza, D. Vanderbilt, and N. Marzari, [Comput. Phys. Commun. **178**, 685 \(2008\)](#).
- [62] A. Jain, S. P. Ong, G. Hautier, W. Chen, W. D. Richards, S. Dacek, S. Cholia, D. Gunter, D. Skinner, G. Ceder, and K. A. Persson, [APL Mater. **1**, 011002 \(2013\)](#).
- [63] J. P. Perdew, K. Burke, and M. Ernzerhof, [Phys. Rev. Lett. **77**, 3865 \(1996\)](#).